



Supplement of

Tracing ammonia emission sources in California's Salton Sea region: insights from airborne longwave-infrared hyperspectral imaging and ground monitoring

Sina Hasheminassab et al.

Correspondence to: Sina Hasheminassab (sina.hasheminassab@jpl.nasa.gov)

The copyright of individual parts of the supplement might differ from the article licence.

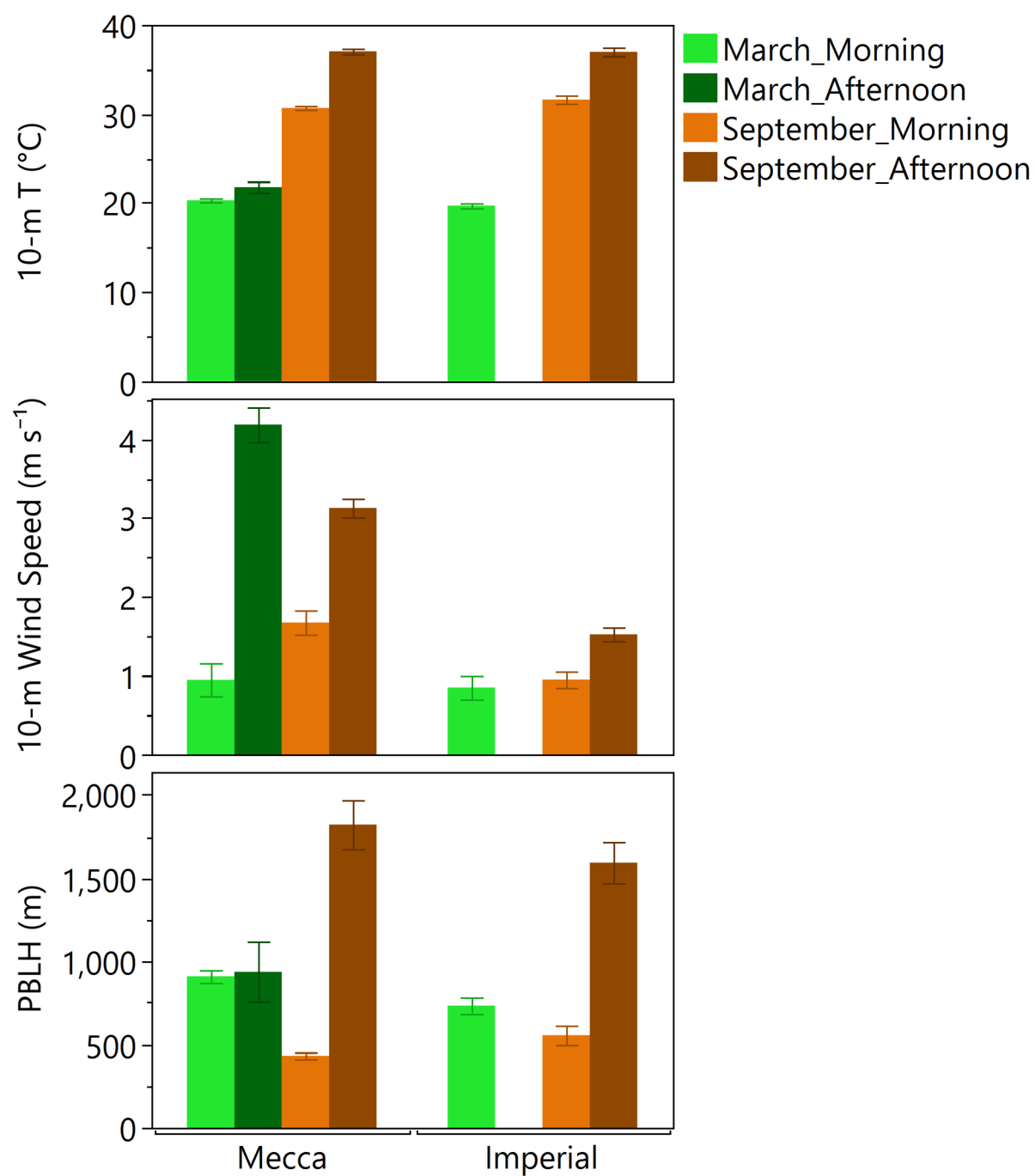


Figure S1. Average temperature and wind speed at 10 m above ground level, and planetary boundary layer height (PBLH) over the Mecca and Imperial study areas during the flight measurement sessions, retrieved from the HRRR model. Error bars represent confidence intervals.

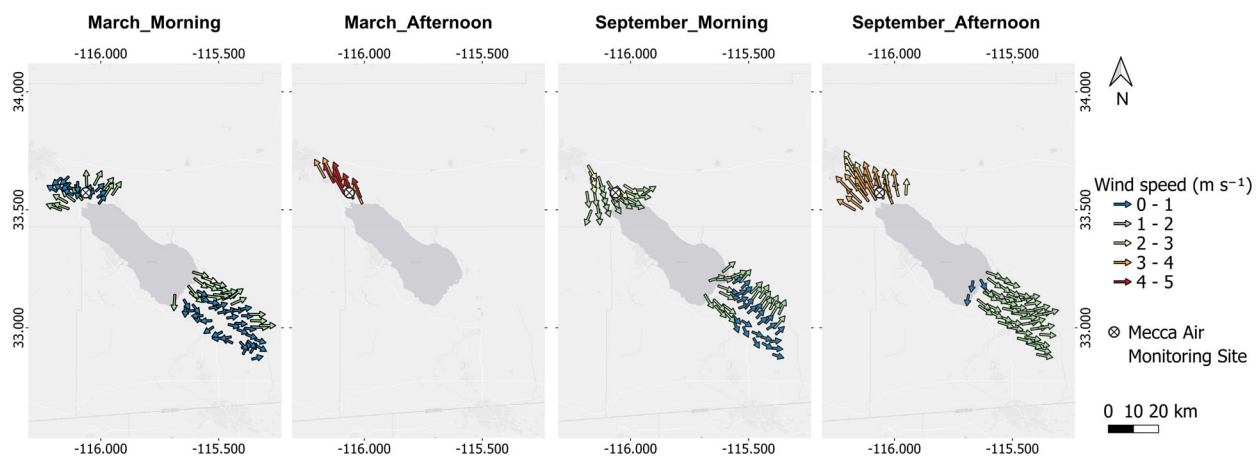


Figure S2. Wind fields at 10 m above ground level over the Mecca and Imperial study areas during flight measurement sessions, retrieved from the HRRR model. Map sources: Sources: Esri, HERE, Garmin, INCREMENT P, ©OpenStreetMap contributors, and the GIS User Community.

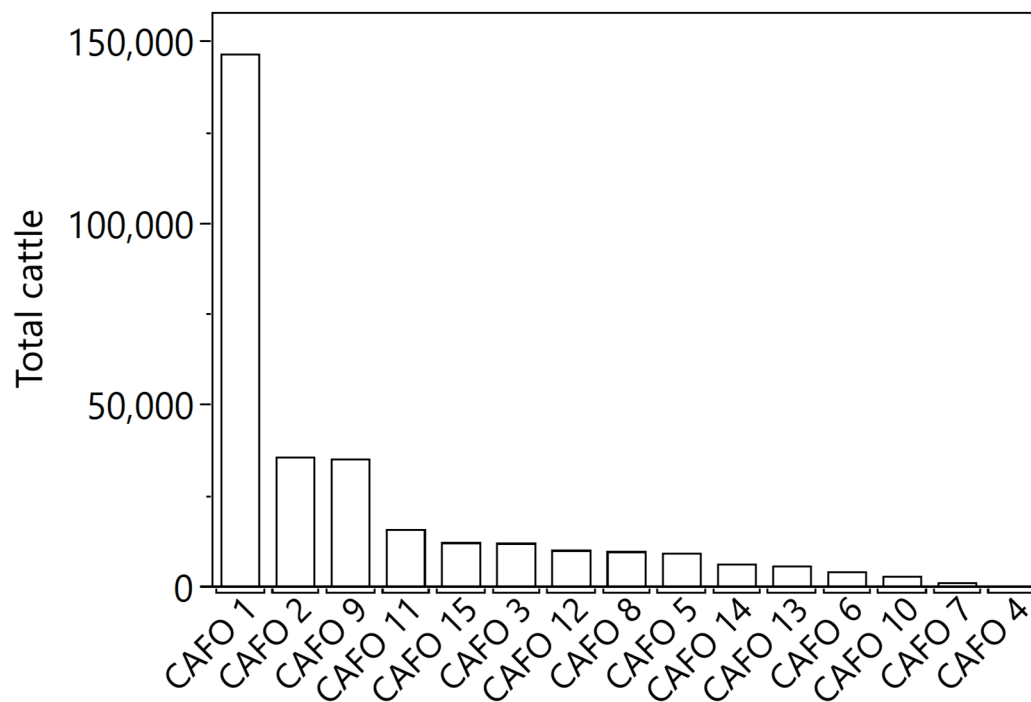


Figure S3. Total cattle population in 2022 at concentrated animal feeding operation (CAFO) facilities in the Imperial study area. Data were obtained from the California Air Resources Board's (CARB) California Dairy & Livestock Database (CADD) (<https://ww2.arb.ca.gov/resources/documents/california-dairy-livestock-database-cadd>, accessed January 4, 2025).

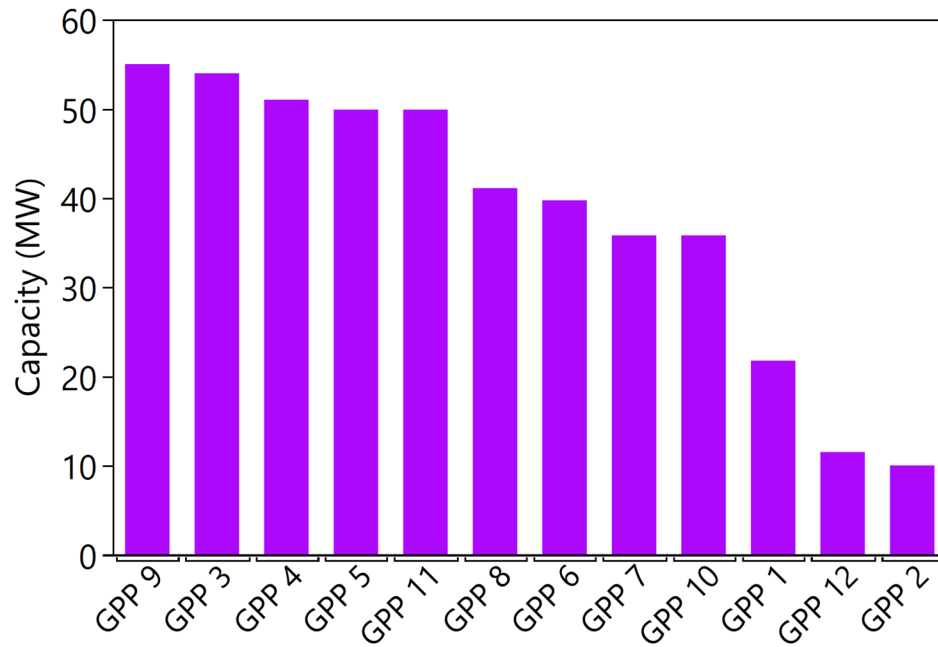


Figure S4. Generating capacity (MW) of geothermal power plants (GPP) in the Imperial study area. Data were obtained from the California State Geoportal (<https://gis.data.ca.gov>, accessed January 4, 2025).

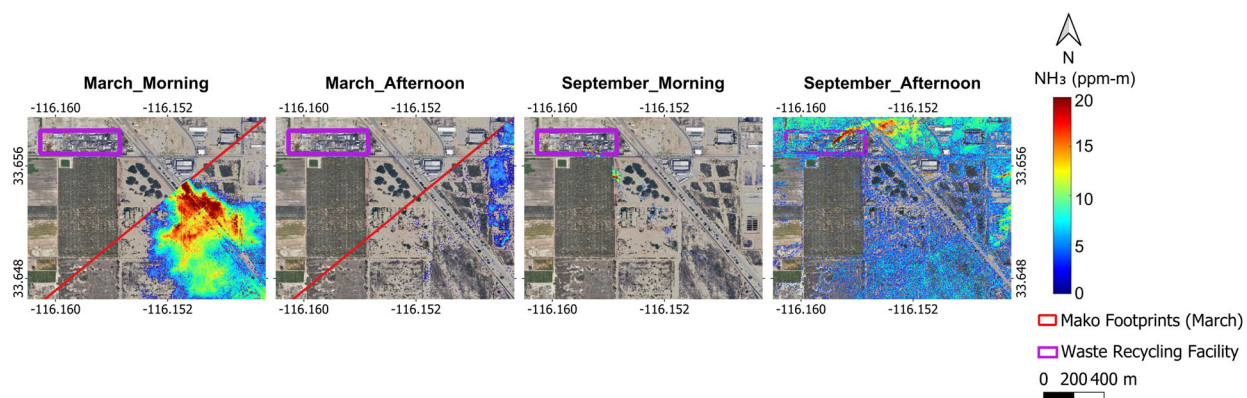


Figure S5. Retrieved NH_3 column density (ppm-m) maps over a waste recycling facility in the Mecca study area during each airborne measurement session. Null pixels that did not meet the t-statistic and ΔT thresholds are rendered transparent. Google Earth imagery is included for reference. Base imagery © Google Earth 2025.

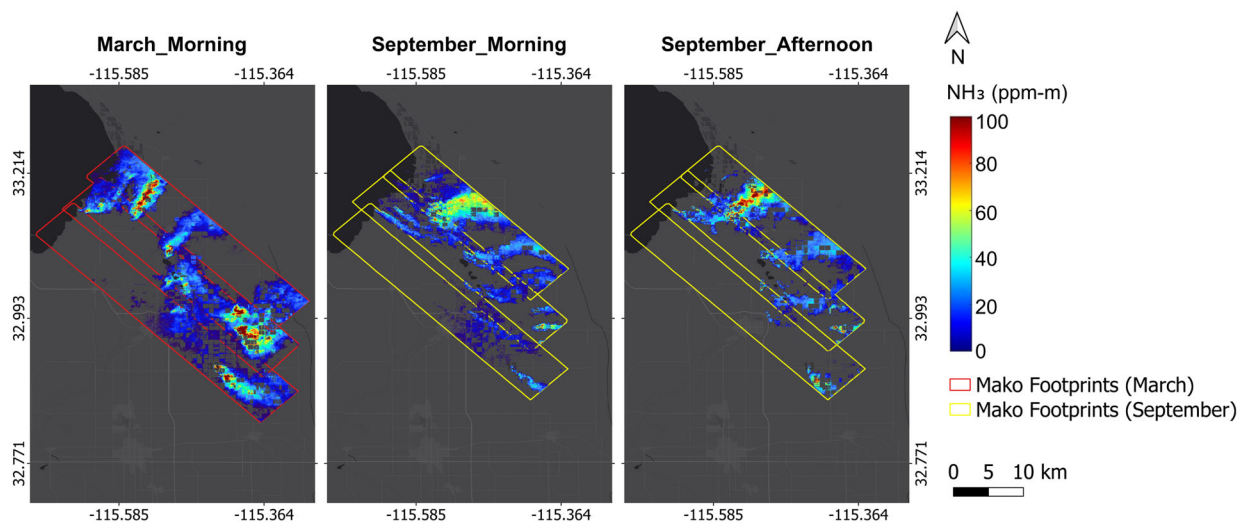


Figure S6. Retrieved NH_3 column density (ppm-m) maps over the Imperial study area during each airborne measurement session. Null pixels that did not meet the t-statistic and ΔT thresholds are rendered transparent. This figure is analogous to Figure 5 but without markers, providing a clearer depiction of the detected plume patterns. Map sources: Esri, HERE, Garmin, INCREMENT P, ©OpenStreetMap contributors, and the GIS User Community.

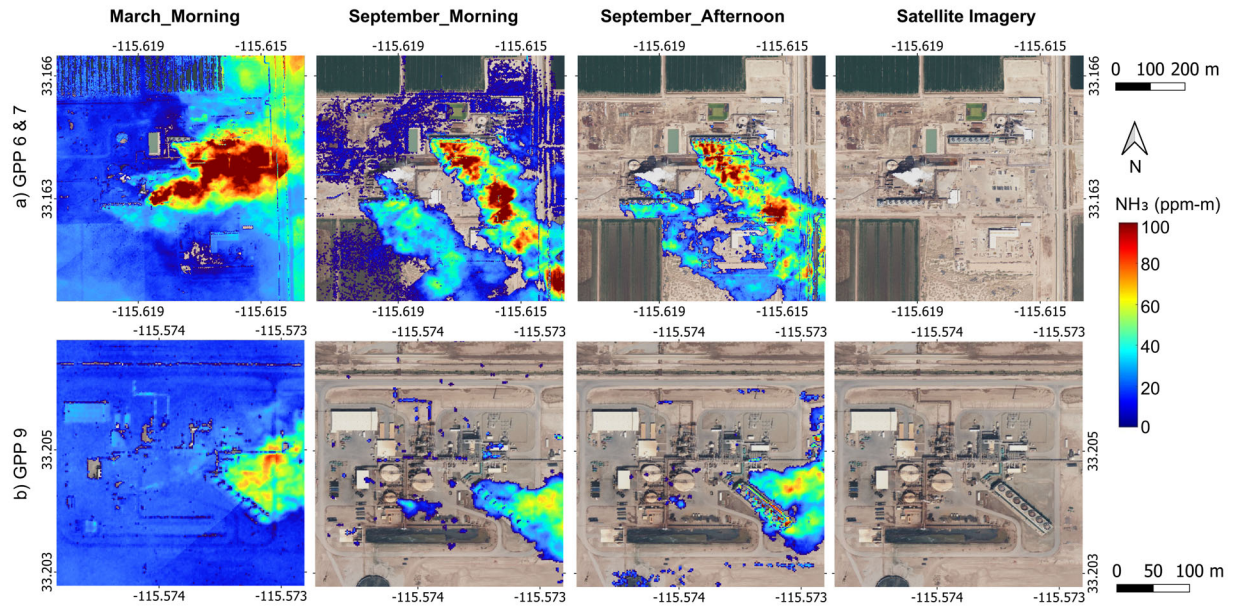


Figure S7 (a-b). Retrieved NH_3 column density (ppm-m) over geothermal power plants (GPP) 6, 7, and 9 in the Imperial study area during each airborne measurement session. Null pixels that did not meet the t-statistic and ΔT thresholds are rendered transparent. Google Earth imagery is included for reference. Base imagery © Google Earth 2025.

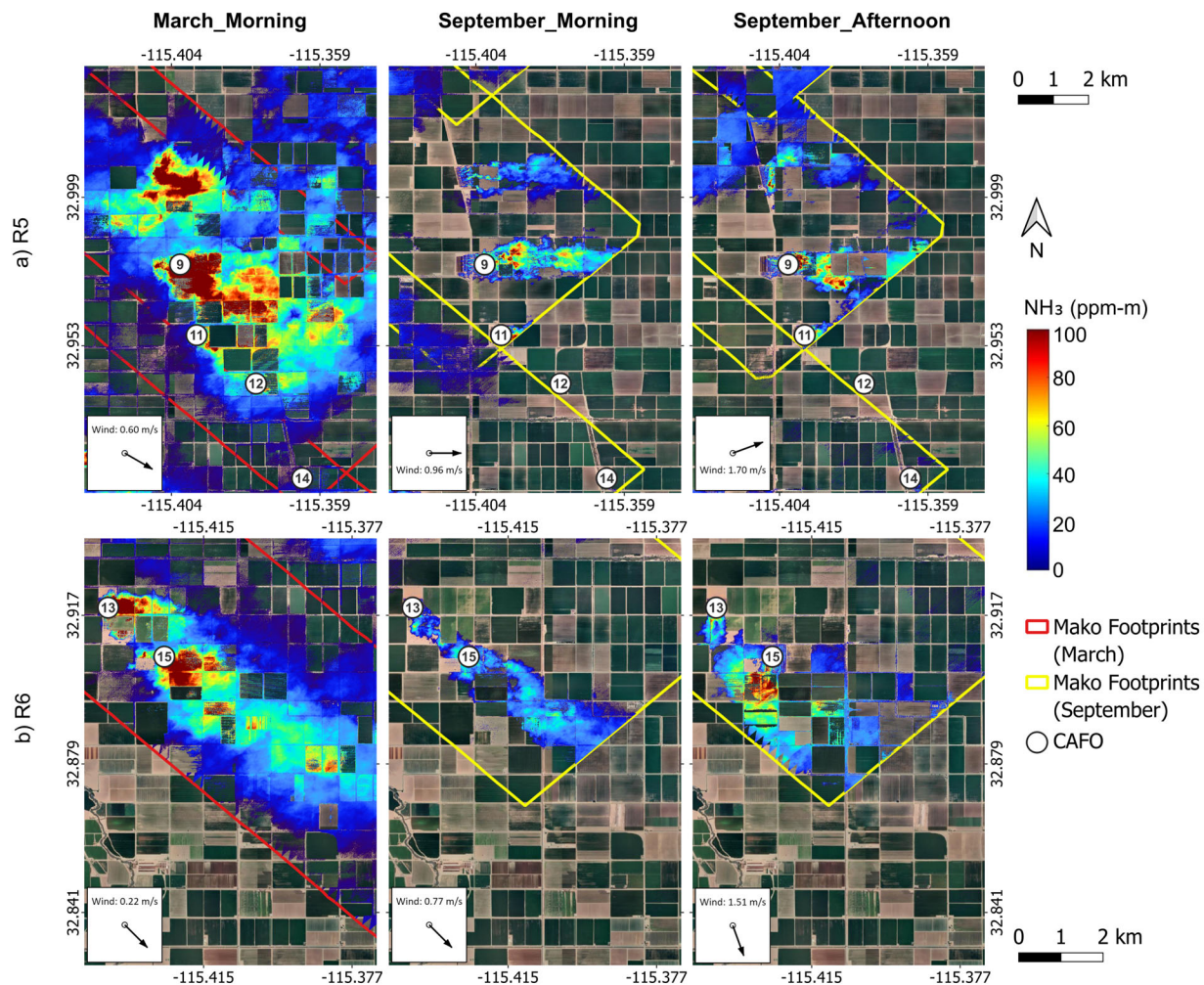


Figure S8 (a-b). Retrieved NH_3 column density (ppm-m) maps over predefined Regions 5–6 in Imperial during each airborne measurement session. Null pixels that did not meet the t-statistic and ΔT thresholds are rendered transparent. Wind directions were inferred from plume patterns, and average wind speeds were calculated from the nearest HRRR grid cells. Google Earth imagery is included for reference. Base imagery © Google Earth 2025.

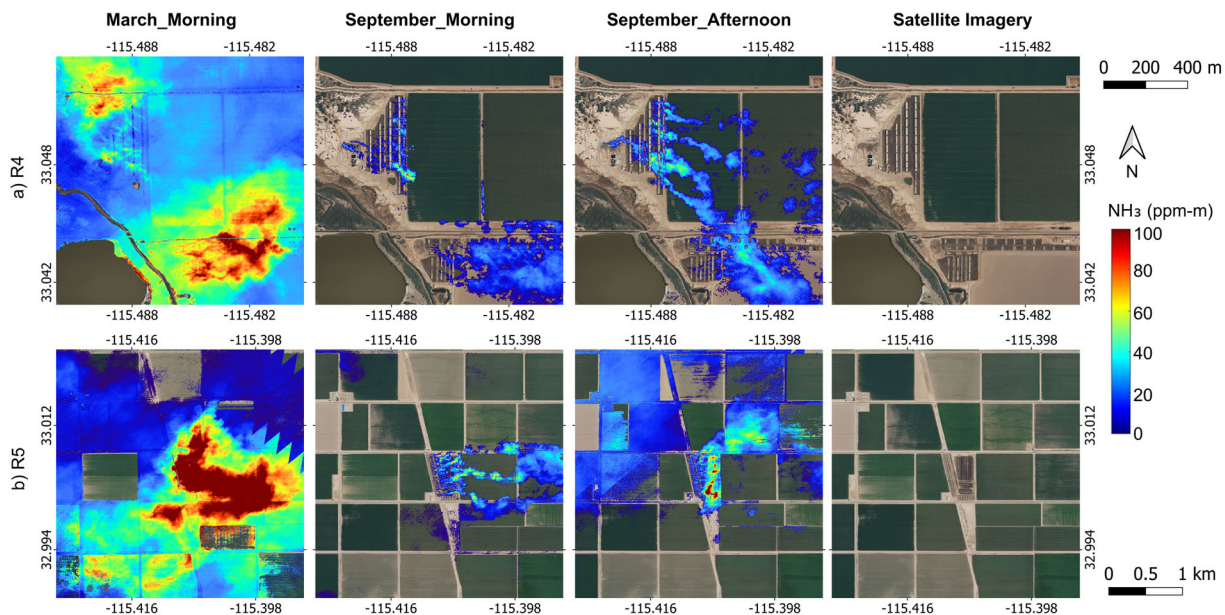


Figure S9 (a-b). Retrieved NH_3 column density (ppm-m) maps over sources not captured in existing records in regions 4 and 5 of the Imperial study area during each airborne measurement session. Null pixels that did not meet the t-statistic and ΔT thresholds are rendered transparent. Google Earth imagery is included for reference. Base imagery © Google Earth 2025.

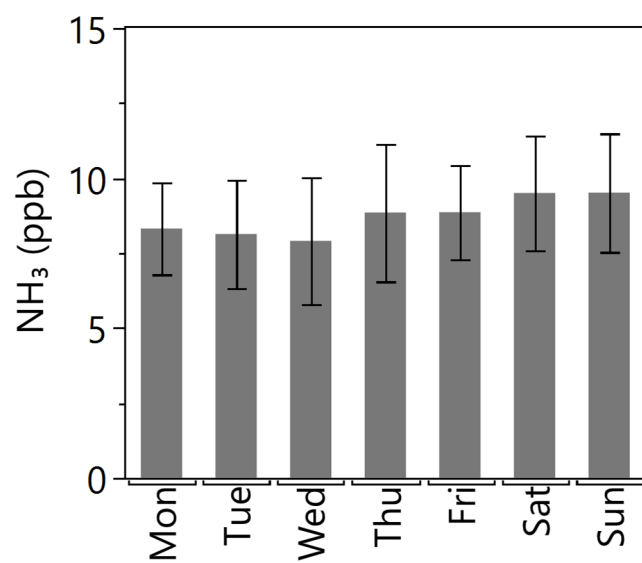


Figure S10. Average ground-level NH_3 concentrations (ppb) for each day of the week in 2023 measured at the Mecca air monitoring site. Error bars represent confidence intervals.

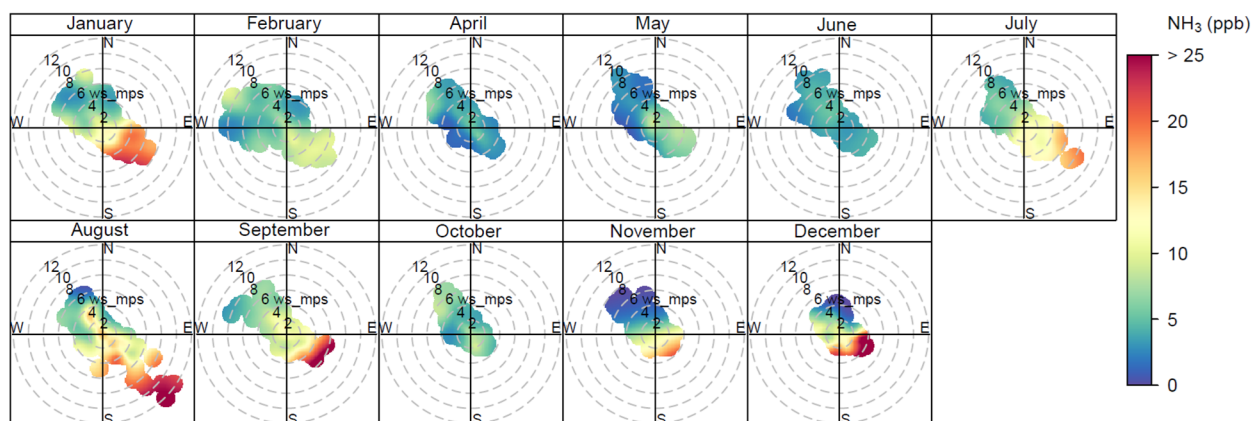


Figure S11. Monthly bivariate polar plots of ground-level NH_3 concentrations (ppb) in 2023, measured at the Mecca air monitoring site. March data is missing due to the NH_3 monitor being non-operational during that period.

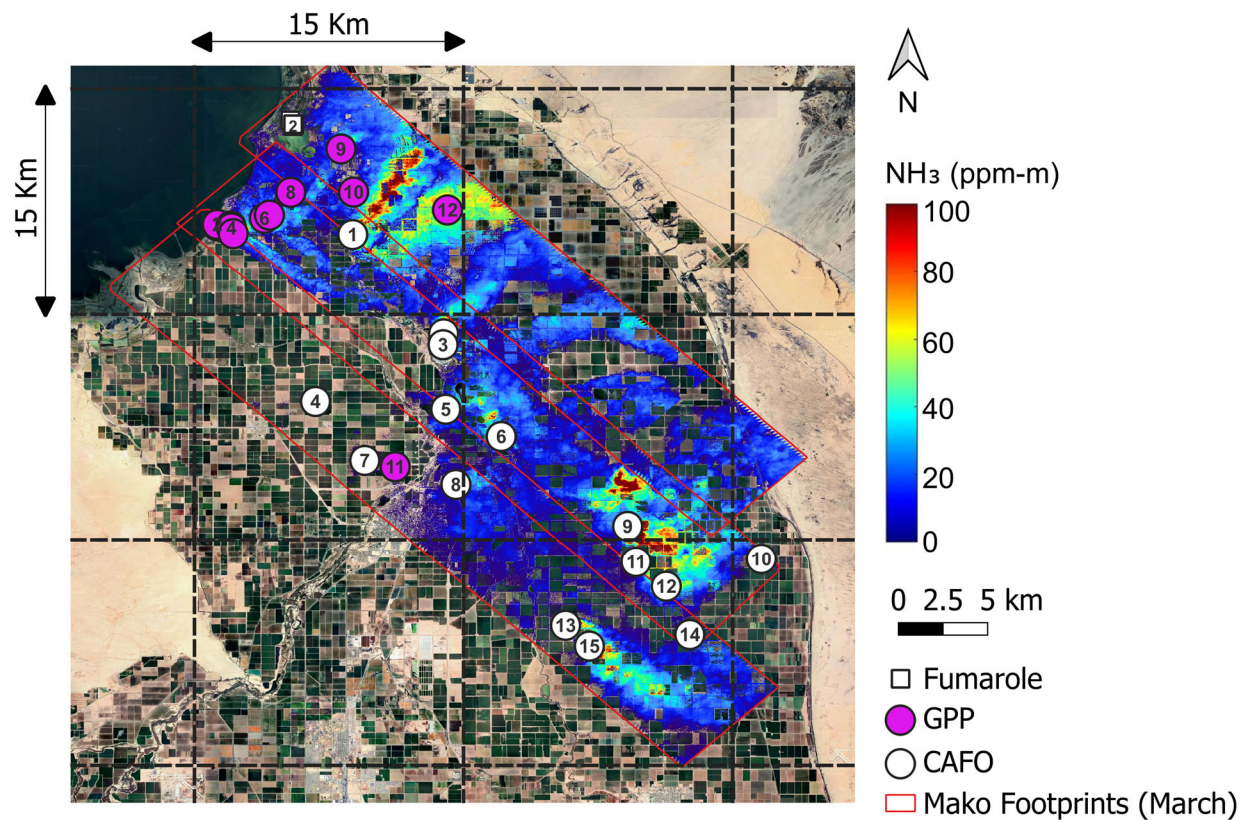


Figure S12. NH_3 column density (ppm-m) map over the Imperial study area on 28 March 2023, overlaid with a hypothetical 15 km x 15 km satellite grid. Base imagery © Google Earth 2025.